

Semi-Blind Multiuser Detection Under the Presence of Reconfigurable Intelligent Surfaces

Nikolaos I. Miridakis, *Senior Member, IEEE*, Theodoros A. Tsiftsis, *Senior Member, IEEE*, Guanghua Yang, *Senior Member, IEEE*, Panagiotis A. Karkazis, and Helen C. Leligou

Abstract

A multiuser multiple-input multiple-output wireless communication system is analytically studied, which operates with the aid of a reconfigurable intelligent surface (RIS). The intermediate RIS is equipped with multiple elements and operates via random phase rotations to simultaneously serve multiple users. Independent Rayleigh fading conditions are assumed among the included channels. The system performance is analytically studied when the linear yet efficient zero-forcing detection is implemented at the receiver. In particular, the outage performance is derived in closed-form expression for different system configuration setups with regards to the available channel state information at the receiver. Further, a joint coherent/noncoherent linear detection is analytically presented. Finally, some new engineering insights are provided, such as how the channel state information and/or the volume of antenna/RIS arrays impact on the overall system performance as well as the arising efficiency on the performance/complexity tradeoff by utilizing the joint coherent/noncoherent scheme.

Index Terms

Corresponding Author: T. A. Tsiftsis.

N. I. Miridakis, T. A. Tsiftsis and G. Yang are with the Institute of Physical Internet and School of Intelligent Systems Science & Engineering, Jinan University, Zhuhai Campus, Zhuhai 519070, China. N. I. Miridakis is also with the Department of Informatics and Computer Engineering, University of West Attica, Aegaleo 12243, Greece (e-mails: nikozm@uniwa.gr, theo_tsiftsis@jnu.edu.cn, ghyang@jnu.edu.cn).

P. A. Karkazis is with the Department of Informatics and Computer Engineering, University of West Attica, Aegaleo 12243, Greece (email: p.karkazis@uniwa.gr).

H. C. Leligou is with the Department of Industrial Design and Production Engineering, University of West Attica, Aegaleo 12241, Greece (email: e.leligkou@uniwa.gr).

Multiple-antenna transmission, multiuser detection, reconfigurable intelligent surfaces (RIS), zero-forcing detection.

I. INTRODUCTION

The reconfigurable intelligent surfaces (RIS), also known as intelligent reflecting metasurfaces, are emerging at the forefront of wireless communications research nowadays [1]–[4]. RISs can control the wireless channel by suitably shifting the phase (and the amplitude response) of the impinging signal on a large number of meta-elements. Doing so, the corresponding reflected signals can be added either constructively or destructively with other signals to enhance the signal-to-noise ratio (SNR) and/or to suppress the co-channel interference at the receiver. Most of the current art is focused on the incident signals' phase shift optimization and/or knowledge acquisition of the channel state information (CSI) at RIS [5]. Nevertheless, such a condition reflects on a considerably high computational complexity and power consumption. In addition, assuming perfect CSI at RIS is challenging, while it may also be infeasible in some practical cases, due to the limited resources and passive nature of RIS deployments. The latter constraints become even more emphatic in multiuser multiple input-multiple output (MIMO) systems [6].

Motivated by the aforementioned observations, in this letter, the performance of a multiuser MIMO communication system is analyzed, which operates with the aid of an intermediate RIS. The linear zero-forcing (ZF) detection is utilized at the receiver to recover the simultaneously detected multiple signals. It is assumed that the signals undergo independent Rayleigh fading conditions. The practical scenario of a fully-blind RIS (in terms of the multiuser CSI) is considered, whereas it is assumed that the phases of RIS elements are randomly rotated so as to serve a set of arbitrarily located multiple users.

New closed-form expressions with regards to the system outage probability are presented, under different use cases regarding the availability of instantaneous CSI at the receiver side. Moreover, the performance of a joint coherent/noncoherent detection scheme is analytically studied, which shows a remarkable efficiency on the performance/complexity tradeoff at RIS-enabled system setups. Insightfully, it is shown that the presence of partial-only CSI (which occurs whenever the CSI of at least one of the three links between transmitter, RIS and receiver is missing) unavoidably produces an SNR-independent outage/error floor. On the other hand, despite the partial CSI assumption, the introduced joint coherent/noncoherent detection effectively tackles this problem even for the suboptimal yet practically feasible random phase rotation

strategy implemented at RIS. Also, the beneficial role of an increased antenna/RIS element array is manifested, while some useful engineering insights are presented. Most importantly, it turns out that utilizing the said joint detection scheme, the arising channel gains reflect on quite a similar performance as the ideal detection scheme (with full CSI of all the included links, yet impractical), but preserving much less computational costs and signaling overhead at the same time.

Notation: Vectors and matrices are represented by lowercase and uppercase bold typeface letters, respectively, whereas \mathbf{I}_v stands for the $v \times v$ identity matrix. A diagonal matrix with entries x_1, \dots, x_n is defined as $\text{diag}\{x_i\}_{i=1}^n$, \mathbf{X}^{-1} is the inverse of \mathbf{X} and \mathbf{X}^\dagger is the Moore-Penrose pseudoinverse of \mathbf{X} . $[\mathbf{X}]_{k,l}$ stands for the entry at the k^{th} row and l^{th} column of \mathbf{X} . Superscript $(\cdot)^H$ denotes Hermitian transposition, $|\cdot|$ represents absolute (scalar) value and $j \triangleq \sqrt{-1}$. $\mathbb{E}[\cdot]$ is the expectation operator, symbol $\stackrel{d}{=}$ means equivalence in distribution and $\stackrel{d}{\asymp}$ defines asymptotic equivalence in distribution. $f_X(\cdot)$ and $F_X(\cdot)$ represent the probability density function (PDF) and cumulative distribution function (CDF) of a random variable (RV) X , respectively. Furthermore, $F_{X|Y}(\cdot|\cdot)$ represents the distribution function of X conditioned on Y . $\mathcal{CN}(\mu, \sigma^2)$ defines a circularly symmetric complex-valued Gaussian RV with mean μ and variance σ^2 ; \mathcal{X}_v^2 stands for a (central) chi-squared RV with v degrees-of-freedom (DoF); while $\mathcal{X}_v^2(u, w)$ denotes that X is a non-central chi-squared RV with v DoF, a non-centrality parameter u and variance w . Also, $\Gamma(\cdot, \cdot)$ denotes the upper incomplete Gamma function [7, Eq. (8.350.2)] and $\Gamma(\cdot)$ denotes the Gamma function [7, Eq. (8.310.1)]. $Q_1(\cdot, \cdot)$ is the first-order Marcum- Q function; ${}_1F_1(\cdot, \cdot; \cdot)$ is the Kummer's confluent hypergeometric function [7, Eq. (9.210.1)]; and $G[\cdot|\cdot]$ represents the Meijer's G -function [7, Eq. (9.301)].

II. SYSTEM AND SIGNAL MODEL

Consider a wireless communication system with M single-antenna transmitters and a receiver equipped with $N \geq M$ antennas¹ operating over a quasi-static block-fading channel. In fact, independent Rayleigh faded channels are assumed which remain fixed for the duration of a given frame transmission while they may change independently amongst various frames. The end-to-end communication is assisted by an RIS equipped with L passive elements. It is also

¹From the analysis presented hereafter, the classical single-user communication scenario with M co-located transmit antennas is included as a special case.

assumed that both the size of each element and the inter-element spacing are equal to half of the signal wavelength; such that the associated channels undergo independent fading [8]. All the given streams are simultaneously transmitted and received via ZF detection.

More specifically, the received signal reads as

$$\mathbf{y} = \sqrt{p}(\mathbf{H}_D + \mathbf{H}\Phi\mathbf{G})\mathbf{s} + \mathbf{n}, \quad (1)$$

where $\mathbf{y} \in \mathbb{C}^{N \times 1}$, p is the transmit SNR and $\mathbf{s} \in \mathbb{C}^{M \times 1}$ is the transmit signal. Also, $\mathbf{H}_D \in \mathbb{C}^{N \times M}$ denotes the channel matrix between the transceiver direct links; $\mathbf{H} \in \mathbb{C}^{N \times L}$ and $\mathbf{G} \in \mathbb{C}^{L \times M}$ are the channel matrices of the RIS-to-receiver and transmitters-to-RIS links, respectively; $\Phi \triangleq \text{diag}\{e^{j\phi_i}\}_{i=1}^L$ denotes the phase rotations at RIS; and $\mathbf{n} \in \mathbb{C}^{N \times 1}$ defines the additive white Gaussian noise at the receiver. Further, it holds that $\mathbf{H}_D \triangleq \mathbf{X}_D \Xi_D^{1/2}$, where $\mathbf{X}_D \in \mathbb{C}^{N \times M}$ and $\mathbf{X}_D \stackrel{d}{=} \mathcal{CN}(\mathbf{0}, \mathbf{I}_N)$, while $\Xi_D \triangleq \text{diag}\{\xi_{D,i}^2\}_{i=1}^M$ with $\xi_{D,i}^2$ standing for the (known) large-scale channel gain of the i^{th} transmitter. In a similar basis, $\mathbf{H} \triangleq \mathbf{X}_H \Xi_H^{1/2}$, $\mathbf{X}_H \in \mathbb{C}^{N \times L}$, $\mathbf{X}_H \stackrel{d}{=} \mathcal{CN}(\mathbf{0}, \mathbf{I}_N)$, and $\Xi_H \triangleq \xi_H^2 \mathbf{I}_L$. Also, $\mathbf{G} \triangleq \mathbf{X}_G \Xi_G^{1/2}$ with $\mathbf{X}_G \in \mathbb{C}^{L \times M}$, $\mathbf{X}_G \stackrel{d}{=} \mathcal{CN}(\mathbf{0}, \mathbf{I}_L)$, and $\Xi_G \triangleq \text{diag}\{\xi_{G,i}^2\}_{i=1}^M$. The gains $\{\xi_{D,i}^2, \xi_{G,i}^2, \xi_H^2\}$ incorporate signal propagation attenuation, antenna gains and shadowing losses, which are assumed either fixed or perfectly known at the receiver.² Lastly, it is assumed that $\mathbb{E}[\mathbf{s}\mathbf{s}^H] = \mathbf{I}_M$ and $\mathbf{n} \stackrel{d}{=} \mathcal{CN}(\mathbf{0}, \mathbf{I}_N)$.

Upon the signal reception, the ZF filter matrix $\mathbf{W} \in \mathbb{C}^{M \times N}$ is applied, yielding to the post-processed signal $\mathbf{r} = \mathbf{W}\mathbf{y}$. The structure of \mathbf{W} depends on the implicit assumption of the known (instantaneous small-scale) channel gains and is further analyzed subsequently.

III. SYSTEM PERFORMANCE

In current work, we study the outage performance of the considered system configuration for different ZF filters \mathbf{W} . For a given SNR of the i^{th} transmitted stream, defined as γ_i , its outage probability is computed as $P_{\gamma_i}(\gamma_{\text{th}}) \triangleq F_{\gamma_i}(\gamma_{\text{th}})$, where $\gamma_{\text{th}} \triangleq 2^R - 1$ is the outage threshold satisfying a target data transmission rate R (in bps/Hz).

²Note that the large-scale RIS-to-receiver channel gains ξ_H^2 are identical for all the involved channel links since the inter-element distance at RIS (or the inter-antenna distance at the receiver) is considered negligible compared to the corresponding RIS-to-receiver distance.

A. Given \mathbf{H}_D , $\mathbf{W} \triangleq \mathbf{H}_D^\dagger$

In this case, the receiver perfectly knows the channel condition of the direct transceiver links, while the individual RIS-enabled channels \mathbf{H} and \mathbf{G} as well as the phase rotations Φ are completely unknown. It holds that

$$\begin{aligned} \mathbf{r} &= \mathbf{H}_D^\dagger [\sqrt{p}(\mathbf{H}_D + \mathbf{H}\Phi\mathbf{G})\mathbf{s} + \mathbf{n}] \\ &= \sqrt{p}\mathbf{s} + \underbrace{\sqrt{p}\mathbf{H}_D^\dagger\mathbf{H}\Phi\mathbf{G}\mathbf{s} + \mathbf{H}_D^\dagger\mathbf{n}}_{\mathbf{n}'_1}, \end{aligned} \quad (2)$$

where \mathbf{n}'_1 denotes the post-processed noise vector with a corresponding covariance matrix being

$$\begin{aligned} &\mathbb{E}[\mathbf{n}'_1(\mathbf{n}'_1)^{\mathcal{H}}] \\ &= p\mathbf{H}_D^\dagger\mathbb{E}[\mathbf{H}\Phi\mathbf{G}\mathbf{G}^{\mathcal{H}}\Phi^{\mathcal{H}}\mathbf{H}^{\mathcal{H}}](\mathbf{H}_D^\dagger)^{\mathcal{H}} + \mathbf{H}_D^\dagger(\mathbf{H}_D^\dagger)^{\mathcal{H}} \\ &= \mathbf{H}_D^\dagger(\mathbf{H}_D^\dagger)^{\mathcal{H}} \left(pL\xi_{\mathbf{H}}^2 \sum_{i=1}^M \xi_{\mathbf{G},i}^2 \right) + \mathbf{H}_D^\dagger(\mathbf{H}_D^\dagger)^{\mathcal{H}} \\ &= (\mathbf{H}_D^{\mathcal{H}}\mathbf{H}_D)^{-1} \left(pL\xi_{\mathbf{H}}^2 \sum_{i=1}^M \xi_{\mathbf{G},i}^2 + 1 \right), \end{aligned} \quad (3)$$

where we used the fact that \mathbf{H} and \mathbf{G} are mutually independent; $\mathbb{E}[\mathbf{H}\mathbf{H}^{\mathcal{H}}] = L\xi_{\mathbf{H}}^2\mathbf{I}_N$; $\Phi\Phi^{\mathcal{H}} = \mathbf{I}_L$; $\mathbb{E}[\mathbf{G}\mathbf{G}^{\mathcal{H}}] = \sum_{i=1}^M \xi_{\mathbf{G},i}^2\mathbf{I}_L$; and $\mathbf{H}_D^\dagger(\mathbf{H}_D^\dagger)^{\mathcal{H}} = (\mathbf{H}_D^{\mathcal{H}}\mathbf{H}_D)^{-1}$. Thereby, the received SNR of the i^{th} stream becomes

$$\gamma_i = \frac{p}{\left(pL\xi_{\mathbf{H}}^2 \sum_{i=1}^M \xi_{\mathbf{G},i}^2 + 1 \right) \left[(\mathbf{H}_D^{\mathcal{H}}\mathbf{H}_D)^{-1} \right]_{i,i}}. \quad (4)$$

Obviously, even when operating at the high transmit SNR regime, the received SNR does not infinitely grow without any bound, since $\gamma_{p \rightarrow \infty} = \{ (L\xi_{\mathbf{H}}^2 \sum_{i=1}^M \xi_{\mathbf{G},i}^2) [(\mathbf{H}_D^{\mathcal{H}}\mathbf{H}_D)^{-1}]_{i,i} \}^{-1}$, thereby, introducing a certain outage/error floor. It is well-known that γ , as per (4), follows a scaled χ_{N-M+1}^2 distribution with a corresponding outage probability given by [9]

$$P_{\gamma_i}(\gamma_{\text{th}}) = 1 - \frac{\Gamma\left(N - M + 1, \frac{\gamma_{\text{th}}(pL\xi_{\mathbf{H}}^2 \sum_{i=1}^M \xi_{\mathbf{G},i}^2 + 1)}{p\xi_{\mathbf{D},i}^2}\right)}{\Gamma(N - M + 1)}. \quad (5)$$

B. Given $\mathbf{H}\Phi\mathbf{G}$, $\mathbf{W} \triangleq (\mathbf{H}\Phi\mathbf{G})^\dagger$

In this case, the channel gains between the transmitter-RIS-receiver link are perfectly known at the receiver³ (not at RIS), whereas the relevant channel status of the direct link remains unknown (or is absent). Following quite a similar approach as in the previous subsection, we get

$$\begin{aligned} \mathbf{r} &= (\mathbf{H}\Phi\mathbf{G})^\dagger [\sqrt{p} (\mathbf{H}_D + \mathbf{H}\Phi\mathbf{G}) \mathbf{s} + \mathbf{n}] \\ &= \sqrt{p}\mathbf{s} + \underbrace{\sqrt{p} (\mathbf{H}\Phi\mathbf{G})^\dagger \mathbf{H}_D \mathbf{s} + (\mathbf{H}\Phi\mathbf{G})^\dagger \mathbf{n}}_{\mathbf{n}'_2}, \end{aligned} \quad (6)$$

and

$$\begin{aligned} &\mathbb{E} [\mathbf{n}'_2 (\mathbf{n}'_2)^{\mathcal{H}}] \\ &= p (\mathbf{H}\mathbf{G})^\dagger \mathbb{E} [\mathbf{H}_D \mathbf{H}_D^{\mathcal{H}}] [(\mathbf{H}\mathbf{G})^\dagger]^{\mathcal{H}} + (\mathbf{H}\mathbf{G})^\dagger [(\mathbf{H}\mathbf{G})^\dagger]^{\mathcal{H}} \\ &= (\mathbf{H}\mathbf{G})^\dagger [(\mathbf{H}\mathbf{G})^\dagger]^{\mathcal{H}} \left(p \sum_{i=1}^M \xi_{D,i}^2 \right) + (\mathbf{H}\mathbf{G})^\dagger [(\mathbf{H}\mathbf{G})^\dagger]^{\mathcal{H}} \\ &= [(\mathbf{H}\mathbf{G})^{\mathcal{H}} (\mathbf{H}\mathbf{G})]^{-1} \left(p \sum_{i=1}^M \xi_{D,i}^2 + 1 \right). \end{aligned} \quad (7)$$

Notably, Φ is not present at the noise covariance of (7) since, in principle, random phase rotations and reflections do not affect channel gains. Hence, the received SNR yields as

$$\gamma_i = \frac{p}{\left(p \sum_{i=1}^M \xi_{D,i}^2 + 1 \right) \left[[(\mathbf{H}\mathbf{G})^{\mathcal{H}} (\mathbf{H}\mathbf{G})]^{-1} \right]_{i,i}}. \quad (8)$$

Similar to the previous case, the latter SNR is bounded even in the asymptotically high p regions; that is $\gamma_{p \rightarrow \infty} = \{ (\sum_{i=1}^M \xi_{D,i}^2) [[(\mathbf{H}\mathbf{G})^{\mathcal{H}} (\mathbf{H}\mathbf{G})]^{-1}]_{i,i} \}^{-1}$. The received SNR as per (8) can be considered as the product of two independent chi-squared RVs with $N - L + 1$ and $L - M + 1$ degrees-of-freedom, correspondingly. Doing so, its PDF reads as [11, Eq. (26)]

$$\begin{aligned} f_{\gamma_i}(x) &= \frac{\left(p \sum_{i=1}^M \xi_{D,i}^2 + 1 \right)}{(N - M)! (L - M)! p \xi_H^2 \xi_{G,i}^2} \\ &\times G_{0,2}^{2,0} \left[\frac{\left(p \sum_{i=1}^M \xi_{D,i}^2 + 1 \right) x}{p \xi_H^2 \xi_{G,i}^2} \middle| \begin{array}{c} - \\ N - M, L - M \end{array} \right]. \end{aligned} \quad (9)$$

³As an indicative example, the transmitter-RIS-receiver cascaded channel can be evaluated by using conventional channel estimation techniques, such as the linear minimum mean squared error or deep learning approach [10].

Then, utilizing [12, Eq. (2.24.2.2)], the outage probability arises as

$$P_{\gamma_i}(\gamma_{\text{th}}) = \frac{\left(p \sum_{i=1}^M \xi_{\text{D},i}^2 + 1\right) \gamma_{\text{th}}}{(N-M)!(L-M)!p\xi_{\text{H}}^2\xi_{\text{G},i}^2} \times G_{1,3}^{2,1} \left[\frac{\left(p \sum_{i=1}^M \xi_{\text{D},i}^2 + 1\right) \gamma_{\text{th}}}{p\xi_{\text{H}}^2\xi_{\text{G},i}^2} \middle| \begin{matrix} 0 \\ N-M, L-M, -1 \end{matrix} \right]. \quad (10)$$

C. Given $\mathbf{H}_{\text{D}} + \mathbf{H}\Phi\mathbf{G}$, $\mathbf{W} \triangleq (\mathbf{H}_{\text{D}} + \mathbf{H}\Phi\mathbf{G})^\dagger$

This scenario reflects on the ideal condition when the receiver perfectly knows the status of all the included channel fading links, which may serve as a performance benchmark. Unfortunately, the explicit formation of \mathbf{W} renders the problem not amenable for further analysis in terms of an exact and closed-form outage expression. Nonetheless, keeping in mind that $L \gg 1$ in the vast majority of RIS deployments (typically, the number of passive reflecting elements is moderately high in realistic scenarios) and adopting the Lyapunov central limit theorem, we can easily show that⁴

$$\mathbf{H}\Phi\mathbf{G} \stackrel{\text{d}}{\simeq} \mathbf{A}\Psi^{1/2}, \text{ as } L \rightarrow \infty, \quad (11)$$

where $\mathbf{A} \stackrel{\text{d}}{=} \mathcal{CN}(\mathbf{0}, \mathbf{I}_N)$ and $\Psi = \text{diag}\{\xi_{\text{H}}^2\xi_{\text{G},i}^2/L\}_{i=1}^M$. Therefore, we proceed by letting the ZF filter be $\mathbf{W} \triangleq (\mathbf{H}_{\text{D}} + \mathbf{H}\Phi\mathbf{G})^\dagger \approx (\mathbf{H}_{\text{D}} + \mathbf{A}\Psi^{1/2})^\dagger$, while the detected signal is approached by

$$\mathbf{r} \approx \sqrt{p}\mathbf{s} + \underbrace{(\mathbf{H}_{\text{D}} + \mathbf{A}\Psi^{1/2})^\dagger}_{\mathbf{n}'_3} \mathbf{n}. \quad (12)$$

Hence, the received SNR in this case yields as

$$\gamma_i \approx \frac{p}{\left\{ \left[(\mathbf{H}_{\text{D}} + \mathbf{A}\Psi^{1/2})^{\mathcal{H}} (\mathbf{H}_{\text{D}} + \mathbf{A}\Psi^{1/2}) \right]^{-1} \right\}_{i,i}}. \quad (13)$$

Since both \mathbf{H}_{D} and \mathbf{A} are mutually independent with zero-mean circularly symmetric complex-Gaussian entries while Ψ has a diagonal structure, the corresponding outage probability has a well-known form and is directly expressed as

$$P_{\gamma_i}(\gamma_{\text{th}}) \approx 1 - \frac{\Gamma\left(N-M+1, \frac{\gamma_{\text{th}}}{p\left(\xi_{\text{D},i}^2 + \frac{\xi_{\text{H}}^2\xi_{\text{G},i}^2}{L}\right)}\right)}{\Gamma(N-M+1)}. \quad (14)$$

⁴In principle, it is required that $L \rightarrow \infty$. However, it has been shown in the literature (e.g., see [13]) that (11) still holds even for moderate L ranges (say, $L \geq 16$). This will be numerically verified in the next Section.

D. Joint coherent/noncoherent detection

Consider the reasonable scenario when the receiver knows the channel status of the direct link and knows nothing about the (instantaneous) RIS-enabled small-scale channel fading. The received signal here is identical to (2). Yet, it is convenient for performance analysis reasons to follow an alternative approach by adopting the QR decomposition of the given channel fading matrix. Specifically, let $\mathbf{H}_D \triangleq \mathbf{Q}\mathbf{R}$, where \mathbf{Q} and \mathbf{R} denote an $N \times N$ unitary matrix (with its columns representing the orthonormal ZF nulling vectors) and $N \times M$ upper triangular matrix, respectively. Then, $\mathbf{W} = \mathbf{Q}^H$ and the received signal becomes

$$\begin{aligned} \mathbf{r} &= \mathbf{Q}^H [\sqrt{p}(\mathbf{H}_D + \mathbf{H}\Phi\mathbf{G})\mathbf{s} + \mathbf{n}] \\ &= \sqrt{p}(\mathbf{R} + \mathbf{Q}^H\mathbf{H}\Phi\mathbf{G})\mathbf{s} + \mathbf{Q}^H\mathbf{n} \\ &\approx \sqrt{p}(\mathbf{R} + \mathbf{Q}^H\mathbf{A}\Psi^{1/2})\mathbf{s} + \mathbf{Q}^H\mathbf{n}, \end{aligned} \quad (15)$$

where the last approximation implies that $L \gg 1$ by referring back to (11). By closely observing (15), the (unknown) RIS-enabled channel term $\mathbf{H}\Phi\mathbf{G}$ s carries transmit symbol information; thus, it can be treated as *a signal rather than (colored) noise*. To this end, prior to symbol decoding, the post-detected signal in (15) passes through a simple noncoherent detector (e.g., envelope detection) such that the received SNR of the i^{th} stream reads as

$$\gamma_i \approx \frac{p |\mathbf{R} + \mathbf{Q}^H\mathbf{A}\Psi^{1/2}|_{i,i}^2}{\mathbf{Q}^H\mathbb{E}[\mathbf{nn}^H]\mathbf{Q}} \stackrel{\text{d}}{=} p |\mathbf{R} + \mathbf{A}\Psi^{1/2}|_{i,i}^2. \quad (16)$$

According to the unitary property applied on zero-mean Gaussian vectors [14, Thm. 1.5.5], i.e., $\mathbf{Q}^H\mathbf{n} \stackrel{\text{d}}{=} \mathbf{n}$ and $\mathbf{Q}^H\mathbf{A} \stackrel{\text{d}}{=} \mathbf{A}$, the derived SNR expression in (16) is accurate and reveals a clear physical meaning. Particularly, in most practical system setups, RIS-enabled channel links may be much more impactful than the direct transmitter-receiver ones (say, much shorter distances), which in turn pronounce the contribution of the $\mathbf{H}\Phi\mathbf{G}$ s signal term to the overall system performance more emphatically in comparison to the conventional approach.

Given \mathbf{H}_D (and, thus, \mathbf{R}), the received SNR of the i^{th} stream as per (16) is distributed as $\gamma_i \stackrel{\text{d}}{=} \chi_2^2(p|r_{i,i}|^2, \sigma_i^2)$, where $r_{i,j}$ is the entry at the i^{th} row and j^{th} column of \mathbf{R} as well as $\sigma_i^2 \triangleq p\xi_H^2\xi_G^2/(2L)$. It follows that

$$P_{\gamma_i|p|r_{i,i}|^2}(\gamma_{\text{th}}|y) \approx 1 - Q_1\left(\sqrt{\frac{y}{\sigma_i^2}}, \sqrt{\frac{\gamma_{\text{th}}}{\sigma_i^2}}\right), \quad (17)$$

with $f_{p|r_{i,i}|^2}(y) = y^{N-M} \exp(-y/p\xi_{D,i}^2)/[(N-M)!(p\xi_{D,i}^2)^{N-M+1}]$. Finally, the unconditional outage probability of the i^{th} stream is derived by

$$\begin{aligned}
P_{\gamma_i}(\gamma_{\text{th}}) &\approx \int_0^\infty P_{\gamma_i||r_{i,i}|^2}(\gamma_{\text{th}}|y) f_{|r_{i,i}|^2}(y) dy \\
&= 1 - \exp\left(-\frac{L\gamma_{\text{th}}}{p\xi_{H,i}^2\xi_{G,i}^2}\right) \left[1 + \sum_{l=0}^{N-M} \frac{L^2\gamma_{\text{th}} \left(\frac{L\xi_{D,i}^2}{\xi_{H,i}^2\xi_{G,i}^2} + 1\right)^{-l}}{Lp\xi_{H,i}^2\xi_{G,i}^2 + \frac{p(\xi_{H,i}^2\xi_{G,i}^2)^2}{\xi_{D,i}^2}} \right. \\
&\quad \left. \times {}_1F_1\left(l+1; 2; \frac{L^2\gamma_{\text{th}}}{Lp\xi_{H,i}^2\xi_{G,i}^2 + \frac{p(\xi_{H,i}^2\xi_{G,i}^2)^2}{\xi_{D,i}^2}}\right) \right], \tag{18}
\end{aligned}$$

where the latter result is obtained by utilizing [15, Eq. (12)] and after some straightforward manipulations.⁵

E. Engineering Insights and Outcomes

In practice, the considered approach can be realized in the uplink of a (distributed) MIMO system operating with the aid of an intermediate RIS. The independent Rayleigh fading assumption is valid whenever a dominant (line-of-sight) channel link is absent within a rich-scattering environment; e.g., in a dense outdoor urban terrestrial. The considered spatial multiplexing approach relies on the fact that $N \geq L \geq M$, which in various cases it holds that $N \geq L \gg M$ (for instance in massive MIMO deployments). For such a system setup, the channel is usually being estimated via pilot signaling prior to the data communication phase. Eventually, it turns out that the pilot length reaches to [17] $NLM + NM$ channel uses (i.e., time instances), which requires rather long pilot sequences; especially for quite large $\{N, L\}$ arrays. This process is time-consuming and may even do not comply with fundamental boundaries, such as the transmission block coherence time interval, which renders the problem quite challenging and prohibitive for practical applications [1].

On another front, in current work, we adopt the conventional channel status acquisition between (only) the direct transmitter/receiver faded links, while the RIS elements employ random rotations. We capitalize on the indirect impact caused by the channel gain of the RIS-enabled

⁵Typically, ${}_1F_1(\cdot)$ is an infinite series representation. Fortunately, in this certain case, the said function includes integer-valued parameters. Therefore, it can be reduced to a finite series representation with the aid of [16, Eqs. (07.20.03.0026.01) and (07.20.03.0025.01)] including elementary-only functions. Doing so, (18) denotes an efficient closed-form expression of the considered system outage performance.

links in a noncoherent yet practically feasible basis. It is noteworthy that when adopting the considered approach, the length of pilot symbols is only NM , which is a viable solution. In addition, an outage/error floor is evident when partial CSI is available (either of the direct or RIS link). On the other hand, the received SNR grows unboundedly only when full CSI is available (ideal case, hard to implement) or when adopting the joint coherent/noncoherent approach. Next section cross-compares the performance of the above schemes and manifests the efficiency of the performance/complexity tradeoff provided by the considered semi-blind joint detection scheme.

IV. NUMERICAL RESULTS AND CONCLUDING REMARKS

In this section, the derived analytical results are verified via numerical validation, whereas they are cross-compared with corresponding Monte-Carlo simulations. Also, without loss of generality and for the sake of clarity, hereinafter, we assume an identical statistical profile for each transmitted stream (i.e., $\xi_{D,i}^2 \triangleq \xi_D^2 \forall i$ and $\xi_{G,i}^2 \triangleq \xi_G^2 \forall i$) in order to evaluate more concretely the overall system performance and obtain more impactful insights. In what follows, line-curves and solid dot-marks denote the analytical and simulation results, respectively. Labels ‘*D*’, ‘*RIS*’, ‘*D+RIS*’, and ‘*Joint*’ correspond, respectively, to the cases when CSI is known only for the direct link, RIS link, direct and RIS links, as well as the joint coherent/noncoherent approach with only the direct link known. Finally, we set $R = 3$ bps/Hz.

In Fig. 1, the system outage performance is illustrated vs. various transmit SNR regions with a particular emphasis on the relatively low SNR regime. The multiuser case of $M = 12$ independent transmitted streams is modeled under large arrays of $N = 32$ receive antennas and either $L = 16$ or $32(= N)$ RIS elements. Obviously, the detrimental effect of the partial CSI (present at the ‘*D*’ and ‘*RIS*’ cases) appears due to the unavoidable outage/error floor. Most importantly, the performance difference between the full-CSI (coherent detection) ‘*D+RIS*’ approach against to the noncoherent joint approach is quite small (less than 1dB), while it is being reduced for an increasing number of RIS elements.

In Fig. 2, the system outage performance is illustrated for various target data rates, when the large-scale channel gain of the direct link, ξ_D^2 , is equal or less to the individual RIS-enabled channel gains, correspondingly. This implies longer (at least equal) distances of the direct transceiver links in comparison to the individual RIS-enabled ones. As expected, the performance gets worse for an increased R and reduced ξ_D^2 . It is verified again that the coherent scheme slightly outperforms the corresponding joint approach at the expense of a considerably

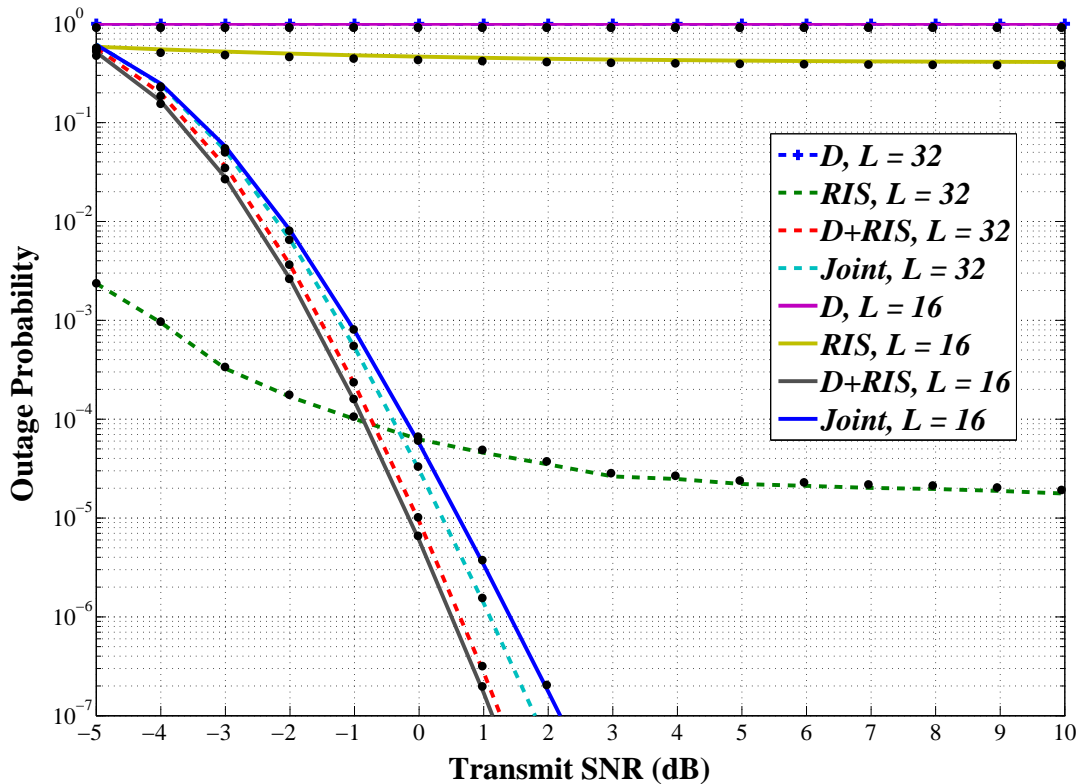


Fig. 1. Outage probability vs. various transmit SNR values and different RIS arrays, when $M = 12$ and $N = 32$. Also, it is assumed that $\{\xi_D^2, \xi_G^2, \xi_H^2\} = 1$.

higher computational overhead. Furthermore, the suboptimal approach under perfect CSI in [17] is presented for performance comparison reasons. In fact, [17, Algorithm 1] introduces a joint optimization method of both power transmission and phase alignment at RIS. However, only the phase optimization is implemented in Fig. 2 (for a fair comparison to the proposed approach), as per [17, Eq. (23)]. Notably, the suboptimal scheme in [17] outperforms the considered random-phase approach; yet, at the cost of an increased computational complexity and a considerably higher signaling overhead ($NLM + NM$ against only NM provided by the proposed random-phase approach).

Overall, the outcomes derived from Figs. 1 and 2 are encouraging since the joint detection scheme comes with a significant reduction of the signaling (pilot) overhead which is in the order of NLM ; whereby, it reflects a notable gain especially in massive MIMO deployments with large RIS arrays. Such a beneficial feature is achieved by introducing a manageable computational burden via a cost-efficient hardware gear for the noncoherent detection so as to capture the

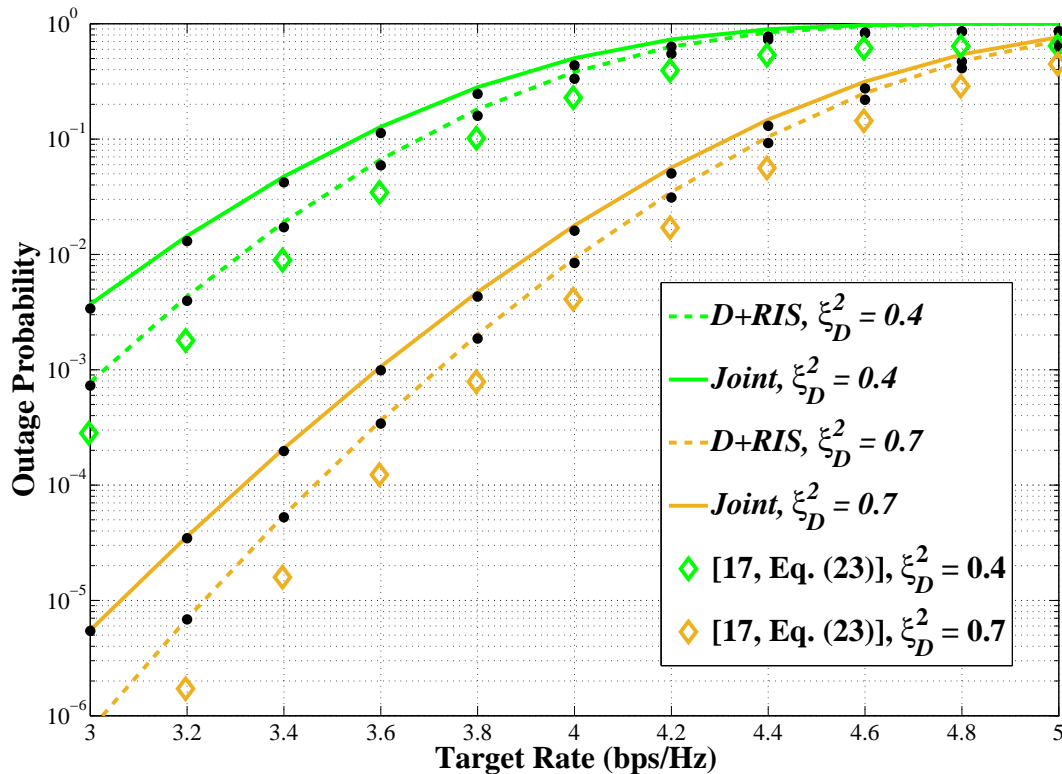


Fig. 2. Outage probability vs. different target data rates, where $N = 32$, $M = 14$ and $L = 16$. Also, it is assumed that $\xi_H^2 = \xi_G^2 = 0.7$, while $p = 3\text{dB}$.

RIS-enabled channel gains.

REFERENCES

- [1] Z. Wang, L. Liu, and S. Cui, "Channel estimation for intelligent reflecting surface assisted multiuser communications: Framework, algorithms, and analysis," *IEEE Trans. Wireless Commun.*, vol. 19, no. 10, pp. 6607–6620, Oct. 2020.
- [2] X. Qian, M. Di Renzo, J. Liu, A. Kammoun, and M.-S. Alouini, "Beamforming through reconfigurable intelligent surfaces in single-user MIMO systems: SNR distribution and scaling laws in the presence of channel fading and phase noise," *IEEE Wireless Commun. Lett.*, vol. 10, no. 1, pp. 77–81, Jan. 2021.
- [3] Y. Zhang, J. Zhang, M. D. Renzo, H. Xiao, and B. Ai, "Performance analysis of RIS-aided systems with practical phase shift and amplitude response," *IEEE Trans. Veh. Technol.*, vol. 70, no. 5, pp. 4501–4511, May 2021.
- [4] C. Psomas and I. Krikidis, "Low-complexity random rotation-based schemes for intelligent reflecting surfaces," *IEEE Trans. Wireless Commun.*, vol. 20, no. 8, pp. 5212–5225, Aug. 2021.
- [5] P. Dharmawansa, S. Atapattu, and M. D. Renzo, "Performance analysis of a two-tile reconfigurable intelligent surface assisted 2×2 MIMO system," *IEEE Wireless Commun. Lett.*, vol. 10, no. 3, pp. 493–497, 2021.
- [6] A. Khaleel and E. Basar, "Reconfigurable intelligent surface-empowered MIMO systems," *IEEE Syst. J.*, vol. 15, no. 3, Sep. 2021.
- [7] I. S. Gradshteyn and I. M. Ryzhik, *Table of Integrals, Series, and Products*. Academic Press, 2007.

- [8] M. Di Renzo, A. Zappone, M. Debbah, M.-S. Alouini, C. Yuen, J. de Rosny, and S. Tretyakov, "Smart radio environments empowered by reconfigurable intelligent surfaces: How it works, state of research, and the road ahead," *IEEE J. Sel. Areas Commun.*, vol. 38, no. 11, pp. 2450–2525, Nov. 2020.
- [9] D. A. Gore, R. W. Heath, and A. J. Paulraj, "Transmit selection in spatial multiplexing systems," *IEEE Commun. Lett.*, vol. 6, no. 11, pp. 491–493, Nov. 2002.
- [10] N. K. Kundu and M. R. McKay, "Channel estimation for reconfigurable intelligent surface aided MISO communications: From LMMSE to deep learning solutions," *IEEE Open J. Commun. Soc.*, vol. 2, pp. 471–487, 2021.
- [11] M. Kieburg, G. Akemann, G. Alfano, and G. Caire, "Closed-form performance analysis of linear MIMO receivers in general fading scenarios," in *23rd Int. ITG Workshop on Smart Ant.*, 2019, pp. 1–7.
- [12] A. P. Prudnikov, Y. A. Brychkov, and O. Marichev, *Integrals and Series, vol 3: more special functions*. Gordon and Breach science publishers, 1986.
- [13] M.-A. Badiu and J. P. Coon, "Communication through a large reflecting surface with phase errors," *IEEE Wireless Commun. Lett.*, vol. 9, no. 2, pp. 184–188, Feb. 2020.
- [14] R. J. Muirhead, *Aspects of Multivariate Statistical Theory*. New York: John Wiley & Sons, 1982.
- [15] P. C. Sofotasios, S. Muhaidat, G. K. Karagiannidis, and B. S. Sharif, "Solutions to integrals involving the Marcum Q -function and applications," *IEEE Signal Process. Lett.*, vol. 22, no. 10, pp. 1752–1756, Oct. 2015.
- [16] I. W. Research, *Mathematica Edition: Version 8.0*. Champaign, Illinois: Wolfram Research, Inc., 2010.
- [17] S. Zhang and R. Zhang, "Capacity characterization for intelligent reflecting surface aided MIMO communication," *IEEE J. Sel. Areas Commun.*, vol. 38, no. 8, pp. 1823–1838, Aug. 2020.